Project FORTE - Nuclear Thermal Hydraulics Research & Development

Smart Component Models for Nuclear Reactors

August 2019

FNC 53798/48650R Issue 1

FRAZER-NASH CONSULTANCY

SYSTEMS AND ENGINEERING TECHNOLOGY

An introduction to Project FORTE

The Department for Business, Energy and Industrial Strategy (BEIS) has tasked Frazer-Nash Consultancy and its partner organisations to deliver the first phase of a programme of nuclear thermal hydraulics research and development.

Phase 1 of the programme comprises two parts:

- The specification and development of innovative thermal hydraulic modelling methods and tools; and
- The specification of a new United Kingdom thermal hydraulics test facility.

The work is intended to consider all future reactor technologies including Gen III+, small modular reactors and advanced reactor technologies.

Our project partners

The team is led by Frazer-Nash Consultancy and includes:

FRAZER-NASH CONSULTANCY

The University Of Sheffield.

EDF ENERGY

Westinghouse

MANCHESTER 1824
The University of Manchester

Science & Technology Facilities Council

For more information, visit www.innovationfornuclear.co.uk/nuclearthermalhydraulics.html

Executive Summary

Safety assessment of a nuclear reactor and its associated components relies strongly on thermal hydraulic analysis. Computational Fluid Dynamics (CFD) and High Performance Computing (HPC) have developed rapidly in the past few decades, making an impact on thermal hydraulics by improving our understanding of complex physics and optimising aspects of component design. However, it is still not feasible to perform routine industrial thermal hydraulics calculations for sub-systems such as a single fuel channel, let alone a complete reactor core, using CFD due to the high computing cost. The current design calculations and safety case development still rely on the traditional 1-D system or sub-channel codes first developed in the 1960s & 1970s. Such methods have become increasingly inadequate for the high demands in safety and efficiency in the development of advanced reactor systems, where reliable predictions of 3-D phenomena and flow transients are of great importance. Consequently, a grand challenge is to develop a reliable and robust, low cost, highly flexible, full 3-D numerical tool for routine engineering calculations taking advantages of the modern advancement in CFD.

The vision of this task is to develop a modern, CFD-based, new-concept sub-channel framework for nuclear power plant design. Our solution is Sub-Channel CFD (SubChCFD).

Sub-channel CFD is based on a standard CFD solver whilst embracing the sub-channel correlations of the current industry standard for model closure. This smart mix of CFD and sub-channel methodologies is able to take advantage of both approaches and, equally importantly, circumventing their drawbacks. Similar to a sub-channel code, SubChCFD is ‘calibratable’ making use of existing engineering data, and can be validated and potentially locked-down and licensed for specific reactor designs. Thanks to its reduced computing cost, compared with tradition CFD approaches, it is possible to provide a full 3-D simulation of very large nuclear systems and the use of a CFD platform allows for areas of local refinement in regions of interest.

SubChCFD uses a two-level mesh system: (i) the filtering mesh, which aligns with the sub-channel mesh of the traditional method, enabling the use of existing engineering correlations to account for the integral wall shear and heat transfer effects, and (ii) the computing mesh, on which a typical CFD solver can be used to resolve the inviscid flow with corrections for diffusion using a simple mixing length turbulence model, which can be calibrated for specific applications.

The development of the baseline model of SubChCFD has been completed and validation has been carried out for a range of test cases, including:

- Fully developed flow and heat transfer in a 5x5 bare fuel bundle and its derivative geometries;
- 3-D complex flow in a locally blocked fuel rod bundle; and
- 3-D flow with inter-channel mixing in a partially blocked 14x14 parallel assembly.

Through these test cases, SubChCFD has demonstrated its ability to predict the frictional losses and heat transfer satisfactorily in complex 3-D flows in rod-bundles, with a computing cost of 2 to 3 orders of magnitude lower than that of resolved CFD.

In the future, it is the intention that SubChCFD will be further developed to broaden its scope of application, including accounting for more complex flow physics, such as buoyancy-driven mixed convection and swirling flows, and coupling with resolved CFD and/or porous media methods for system modelling.

Contents

1 Introduction

1.1 Background

With the increasing global impact of environmental issues, such as global warming and climate change arising from over-consumption of carbon-based fuel, nuclear power will continue to play an important role in energy generation. This is due to its high efficiency in supplying energy and its low emission of greenhouse gases. There are currently about 440 nuclear power plants in operation around the world and over 120 new reactors under construction [1]. Following lessons learned from some major nuclear accidents, especially the most recent one in Fukushima in 2011, the importance of passive cooling and safety margin management is becoming increasingly prominent. In addition to steady-state normal operating conditions, the safety assessment of the modern nuclear system needs to consider a variety of additional scenarios, such as: operational transients (e.g. start-up, and shut-down); anticipated off-design operation (for activities such as refuelling) and a wide variety of postulated fault and accident conditions, to enable fault recovery strategies to be developed and to minimise the risk of a radiological release.

1.2 Nuclear Thermal Hydraulic Modelling Tools

The thermal hydraulic elements of the safety assessment of a nuclear reactor core and its associated components mainly relies on thermal hydraulic analysis of the coolant by means of experimental investigation or numerical simulations [2, 3]. Restricted by the computational power in the 1960s to 1980s, thermal hydraulic simulations were mainly performed using the best-estimate system codes such as RELAP5 [4], ATHLET [5], CATHARE [6] and TRAC [7], and sub-channel codes such as COBRA [8], VIPRE [9] and MATRA [10]. The former are usually used to analyse the overall behaviour of the whole system under different operating conditions, whereas the latter provide a relatively detailed thermal hydraulic analysis at the core level by solving 1-D transport equations based on individual flow passages formed between fuel rods or fuel rods and walls, i.e. the sub-channels.

The transport equations are solved by introducing additional physical closure laws given by empirical correlations, which appear as source terms, accounting for un-resolved physics, such as frictional loss, spacer induced effects, turbulence, inter-channel mixing, and void drifting, etc. As such, the sub-channel analysis codes are able to provide numerical predictions at a resolution of the sub-channel scale, which was state-of-the-art in 1-D approaches at that time. However, it is more and more likely that the traditional 1-D codes will no longer be sufficient in meeting the requirements of modern reactor design and safety case development [11, 12], even if they are still very quick to provide an answer. The large increase in computational power in the past few decades allows the most advanced CFD methods to be used by reactor developers to capture some of the complex 3-D physics of coolant flow in nuclear fuel channels. This has the potential to significantly re-shape future nuclear thermal hydraulic analysis, but realising that potential for reactor development is not without its challenges.

Due to the complex internal structure, the scales of the flow in a nuclear reactor span a large range, varying from sub-millimetre (e.g. secondary flow in fuel assemblies) to meters or even tens of meters (e.g. natural circulation in a loss of coolant accident (LOCA)) [13]. This, therefore, requires the computational domain of a CFD model to be meshed using a fine grid to allow most physical scales to be captured, and it is still not practical to carry out a core-level CFD

simulation due to the prohibitive computing expense even with today's high-performance computing systems.

In addition, the flexible and complex nature of CFD increases the level of expertise needed to use it effectively. The greater complexity and potential for 'user effects' also makes managing the uncertainty in CFD predictions much more challenging than in system and sub-channel codes. The latter are generally 'calibrated' and locked down for the modelling of specific plant, leading to a clear validation envelope and a limited number of user choices. The former is often used to build bespoke models involving a large number of user choices, from the details of the mesh and numerical scheme to the choice of mathematical model for specific phenomena (such as turbulence). The challenges in determining or even bounding the uncertainty are particularly pertinent when thermal hydraulic modelling is used in support of nuclear safety. As a result, the use of CFD in support of nuclear safety is very much in its infancy.

CFD simulations can be carried out for representative sections of a reactor with properly defined boundary conditions to reduce the computing cost by taking advantage of the fact that the core structures are typically spatially periodic in a nuclear reactor. Such an approach has been used by various researchers to carry out CFD analyses for single channels [14 - 17], multiple channels [18 - 23], rod bundle arrays [24 - 30], reactor core sectors [31 - 33], and plena [34, 35], etc. With the experiences accumulated in academia, CFD is further used in industry to optimise the design of some key components of reactors, such as spacer grids of a Pressurised Water-cooled Reactor (PWR) fuel assembly [36, 37]. Among these studies and applications, the wall-function Reynolds-Averaged Navier-Stokes (RANS) methods, especially the k-ε series of turbulence models are often used in early research [14 - 16] or the modelling of large components [31 - 35] as they can provide reasonable predictions at relatively small cost since the near-wall region is not resolved.

However, the methods are no longer satisfactory for cases with complex flow phenomena, such as adverse pressure gradients, vortex shedding, impingement, swirling, and buoyancy influenced flows, etc. In such cases, more sophisticated methods are usually required for better predictions, such as anisotropic Reynolds-Stress Models (RSM) and low Reynolds number RANS or unsteady RANS models in which the boundary layer can be resolved down to the viscous sub-layer using high-resolution near-wall meshes (with the first cell y^+ up to 1.0).

In addition, the state-of-the-art high-fidelity methods, e.g. Large Eddy Simulation (LES) and Direct Numerical Simulation (DNS) have also been used by many researchers in nuclear thermal hydraulics [38 - 40]. Due to the extremely high cost of the latter methods, they cannot be widely used in engineering, especially DNS which is still restricted to simple geometries and low Reynolds numbers. They are normally used to generate benchmark datasets for the development of new turbulence models or as a numerical tool for the fundamental study of turbulence.

1.3 Tool Coupling

Work has been done to make use of the advancement of modern CFD in core-level or even system-level modelling by coupling it with low cost simpler methods. In such approaches, CFD usually takes the role of capturing the complex 3-D flow of the most interesting regions/sections in the reactor system, whilst the rest is described using simplified models. The information exchange between different models is challenging but key for understanding the phenomena, which can be time implicit or explicit and spatially decomposed or overlapped, depending on the method used [41].

In system-level modelling, CFD can be coupled to systems codes to enhance their performance in predicting the complex behaviour of the entire Nuclear Power Plant (NPP) under non-ideal conditions. To date, tremendous efforts have been dedicated to enabling the coupling between CFD and system codes. Anderson et al. [42] analysed a Very High-Temperature Reactor (VHTR) using a coupled RELAP/CFD system where the 3-D flow in the outlet plenum was modelled using CFD. Papukchiev et al. [43] coupled ATHLET and ANSYS CFX, and then validations were done based on a pressure thermal shock related experiment for a PWR. Bury [44] studied a reactor containment system under a LOCA scenario using an in-house system code HEPCAL-AD coupled with ANSYS FLUENT. The natural circulation within an annular channel between an inner steel vessel and the containment wall was simulated using CFD. Bavière et al. [45] simulated a sodium-cooled nuclear system with a coupled simulation of CATHARE2 and Trio_U, which allows energy and momentum feedback from CFD to the system code.

Despite the encouraging progress, there are two challenges in such code couplings. One is the low convergence rate due to the weak coupling, e.g. using time explicit scheme in which the information is only exchanged once at the end of each time step. The other major challenge is that it is difficult to develop a generic methodology that can be used for different pairs of coupling codes.

1.4 Reduced Resolution Models

For core-level modelling, one of the most popular approaches used in the open literature is to couple the porous media model with well-resolved CFD to reduce the computing cost. In some of the cases, porous media is used to describe the fuel assemblies [46 - 49], others also include the plena [50, 51]. Some researchers also developed alternative ways to simplify the core modelling. For example, Corzo et al. [52] incorporated a 1-D finite volume code to account for the complex fuel channels in a full core simulation of a pressurised heavy water reactor. Zhang et al. [53] employed a distributed resistance model to represent the core module of a real PWR geometry, whilst a detailed model was used for the downcomer and the lower plenum. These simplified methods are, to some extent, similar to the sub-channel codes, in which either the flow is forced in a single direction, or the geometry of the fuel rods is not taken into account explicitly. As such, these approaches are not suitable to capture small to medium scale 3-D transient features, for example, the recirculation behind a blockage.

A new interesting area of research is the development of unresolved, coarse grid CFD to enable relatively large flow systems to be simulated at a low cost. Along this line of research, Hu and Fanning [54] introduced a 3-D momentum source term method to simulate anisotropic flows in fuel channels of wire-wrapped bundles without explicitly resolving the geometrical details of the wires with fine meshes. Bieder et al. [55] also studied wire-wrapped bundles using a low-resolution method, but differed from Hu and Fanning in that they simplified the mesh generation by replacing the wire wrap with a spinal fin. Roelofs et al. [56] proposed a method named Low-Resolution Geometry Resolving (LRGR) CFD which captures ‘medium scale’ flow features without a sub-grid model in the case that secondary flows are not important.

Class et al. [57, 58] employed an even coarser mesh in their approach, referred to as Coarse-Grid CFD (CG-CFD), to make the simulation as efficient as sub-channel codes but without depending on experimental data. They solve the Euler equations instead of the Navier-Stokes equations with diffusion effects accounted for using a volumetric force extracted from detailed simulations pre-performed on the same geometry. This approach has to date not been applied to heat transfer where the parametric procedure could be very challenging due to potential coupling between momentum and energy transport. Along a totally new line, Hanna et al [59]

associated the local error arising from grid coarsening to features of the mesh by training a surrogate statistical model with detailed simulation results using state-of-the-art machine learning technology and then tested their method on a 3D lid-driven cavity flow.

1.5 Future Vision

To summarise, although great strides have been made in CFD over the past few decades, which enable many problems previously only tackled by experiments to be solved by means of numerical simulation (thus saving considerable resources), the application of CFD in real-life engineering is still limited by high computing cost and uncertainties introduced by meshing and numerical schemes, user inputs (e.g. initial and boundary conditions), and physical models especially the turbulence models. Additionally, it is usually very difficult to measure and control these uncertainties due to the generality, complexity and flexibility of the method., For these reasons, reactor design and safety assessment in the nuclear industry still largely rely on the traditional methods, despite their shortfalls.

To make use of the modelling techniques achieved in the booming development of CFD for nuclear thermal-hydraulic modelling in this area, especially modelling at system/core level, and to supplement and potentially replace older methods, an effective solution is to re-implement some key concepts of these 1-D methods under the framework of modern CFD. In doing so, the old 1-D tools could be re-visited and modernised to have some CFD-like features and improved flexibility. At the same time, some advantages of the system/sub-channel codes can be retained so as to provide performance that is at least as good as the system/sub-channel codes without a significant increase in computing cost. In addition, due to sharing a unified CFD platform, this kind of approach has the potential to be easily coupled with traditional CFD methods, thus circumventing a number of difficulties and problems encountered in coupling between different platforms.

This research and development task is aimed at developing a CFD-based new concept sub-channel framework. It is intended to be a reliable and robust, low cost, highly flexible, and a full 3-D numerical tool for routine engineering calculations with an objective to bridge the gap between 1-D codes and detailed CFD. Similar to a traditional sub-channel code, the models created using this method are intended to be ‘calibrated’, validated and potentially locked-down and licensed for specific reactor designs.

Following this idea, we present a new approach to CG-CFD in this report. Unlike the methodology of Class [57, 58] and Hanna [59] which is aimed at alleviating the dependence on experiments and empiricism, our method can best be described as a low-resolution CFD using a correlation-based model closure method, in which the experimental and engineering data are used whenever possible. In this method, the inviscid flow with corrections for mixing is solved on a very coarse grid using a standard CFD solver while the empirical correlations of the frictional loss and heat transfer coefficient are used to ensure correct integral effects of the solid walls.

The methodology that has been developed is described in Section 2. The baseline model has been applied to a number of test cases in Section 3. The conclusions of the work to date are summarised in Section 4.

2 Methodology

Fundamentally different from the traditional 1-D approach, the method presented in this report is based on solving the 3-D Navier-Stokes equations, so that it can easily make use of any fully validated CFD code. Due to the use of a very coarse mesh, even the standard wall-function and RANS-based CFD (with the lowest requirement on mesh resolution) cannot be used to produce correct results for the near-wall effects. Hence, the empirical correlations used in sub-channel codes are employed to account for the frictional effect of the wall on the fluid. To achieve this, another mesh system, namely the 'filtering mesh', based on sub-channel divisions is introduced alongside the computing mesh.

The filtering mesh is exactly the same as that used in a typical sub-channel code, so this method is given the name Sub-Channel CFD (SubChCFD). The mapping between the filtering mesh and the computing mesh is then established through geometrical relations so that any physical parameters and field variables stored on the latter can be used directly to produce corresponding sub-channel quantities for the former by spatial averaging using the following equation,

$$\varphi_{sub,j} = \sum_{i \in j} \left(\frac{V_i}{V_{sub,j}} \right) \varphi_i \tag{1}$$

where $\varphi_{sub,j}$ is the sub-channel-level quantity of φ on the j^{th} filtering mesh element, φ_i is the CFD-level quantity of φ on the i^{th} computing mesh element, V_i is the volume of the i^{th} computing mesh element.

These sub-channel quantities can be further used in relevant empirical correlations to work out the sub-channel level frictional loss and heat transfer coefficient which are then distributed back to the computing mesh to close the CFD system. With the advancement of the iteration process, information is continually exchanged between the computing mesh and the filtering mesh, and thus, finally, the CFD solution can be obtained, integrally satisfying the empirical correlations at the sub-channel level. Figure 1 gives the detailed procedure of this approach.

The momentum part of the Navier-Stokes equations to be solved in SubChCFD is shown as follows,

$$\frac{\partial \rho \vec{u}}{\partial t} + \nabla \cdot \rho \vec{u} \otimes \vec{u} = -\nabla p + \nabla \cdot \bar{\sigma} \,. \tag{2}$$

where $\bar{\sigma}$ is the stress tensor including both the viscous and the turbulence contributions. The discrete form is derived by integrating Equation (2) over each computing mesh cell Ω to yield,

$$\begin{aligned} \iiint_{\Omega} \frac{\partial \rho \vec{u}}{\partial t} dV + \oiint_{S} \vec{u} \left(\rho \vec{u} \cdot \vec{n} \right) dA &= -\oiint_{S} \left(\bar{I} p \cdot \vec{n} \right) dA + \oiint_{S} \bar{\sigma} \cdot \vec{n} dA \\ &= -\oiint_{S} \left(\bar{I} p \cdot \vec{n} \right) dA + \iint_{S_w} \bar{\sigma} \cdot \vec{n} dA + \iint_{S_f} \bar{\sigma} \cdot \vec{n} dA \end{aligned}, \tag{3}$$

where $S = S_w \bigcup S_f$.

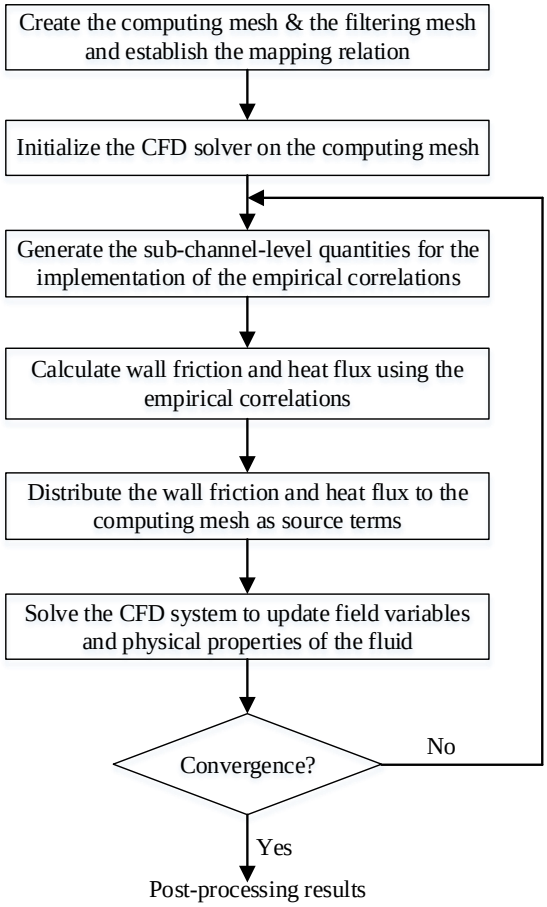

Figure 1: Details of the methodology in the SubChCFD

The convection term in Equation (3) is discretised directly, whereas the viscous term requires some special care. During the Stokes integration, the viscous term can be decomposed into two parts which include the near-wall term and the non-near-wall term, describing viscous forces between the wall and the adjacent fluid element and viscous forces between fluid elements, respectively. Figure 2 shows an example of the mesh system used for a PWR fuel channel where the physical meaning of the two parts of the viscous term is also clearly demonstrated.

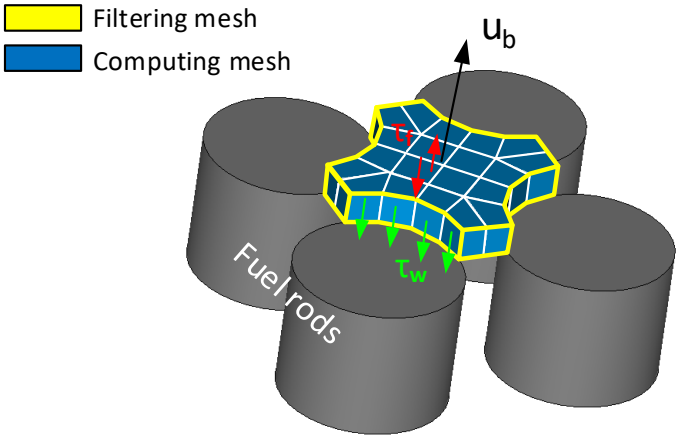

Figure 2: Mesh system in SubChCFD

Since the mesh used in SubChCFD is very coarse, all of the control volumes in the computational domain can be safely assumed to be located in the core flow region with sufficient intensity of turbulence. Therefore, direct discretisation of the non-near-wall term, i.e. the last term in Equation (3), is not expected to have significant errors due to relatively low velocity gradients. The eddy viscosity is then estimated using the 0-equation mixing length turbulence model. As such, the non-near-wall term can be finally written in the following form,

$$\iint_{S_f} \bar{\sigma} \cdot \vec{n} dA = \iint_{S_f} \left(\mu + \mu_t\right)\left(\nabla \vec{u} + \nabla \vec{u}^T - \frac{2}{3}\delta \nabla \cdot \vec{u}\right) \cdot \vec{n} dA, \quad (4)$$

where $\mu_t = \rho l_m^{\ 2} \sqrt{2 S_{ij} S_{ij}}$, the mixing length l_m can be calculated through l_m=0.09δ (δ is the boundary layer thickness, which takes a value of half the hydraulic diameter in bundle flows).

For the near-wall term, i.e. the second last term of Equation (3), can be calculated using the following equation,

$$\iint_{S_W} \bar{\sigma} \cdot \vec{n} dA = -\frac{1}{4} f \frac{1}{2} \rho_{sub} \vec{u}_{sub} \left|\vec{u}_{sub}\right| \iint_{S_W} dA \quad (5)$$

where f denotes the skin fractional factor which differs depending on the specific configuration of a nuclear reactor; ρ_{sub} and $\vec{u}_{sub}$ represent the sub-channel bulk density and bulk velocity, respectively.

Due to the use of the coarse grid, SubChCFD is not expected to achieve complete mesh-independence (even though, as will be shown later in this report, SubChCFD has demonstrated only a small mesh dependence in the case tested). To control this mesh dependence, improve consistency in model generation for different flow problems and improve the accuracy of the simulation, we note the following guidelines on mesh generation for this sub-channel:

1. The filter mesh should be chosen to closely follow the sub-channel divisions used in the specific sub-channel code used to formulate the model closures.
2. The computing mesh should be generated from the filtering mesh, effectively sub-dividing it into smaller cells.
3. Each sub-channel is divided into two regions, namely, the wall region and the core region.
4. We suggest three ‘standard’ mesh strategies as outlined below (refer to Figure 3):
    a. Mesh 1: The wall region is represented by a single wall-layer cell; and the core is meshed by a 2 x 2 mesh.
    b. Mesh 2: The wall region is represented by two wall-layer cells; and the core is meshed by a 2 x 2 mesh.
    c. Mesh 3: The wall region is represented by two wall-layer cells; the core is meshed by a 4 x 4 mesh.

The above mesh strategies allows SubChCFD to have a higher flexibility than the traditional 1-D tools in capturing flow physics. Users can select a proper strategy for computing mesh generation to balance the resulting resolution and computing cost in engineering calculations. In addition, the model parameters used in SubChCFD can be pre-tuned taking into account the mesh strategies to ensure an optimal performance when used for a specific type of nuclear reactor. Figure 3 gives an example of the computing mesh set, including three different resolutions of extruded hexahedron mesh generated in line with the above mesh strategies and a wall-modelled CFD mesh for a square-lattice PWR sub-channel.

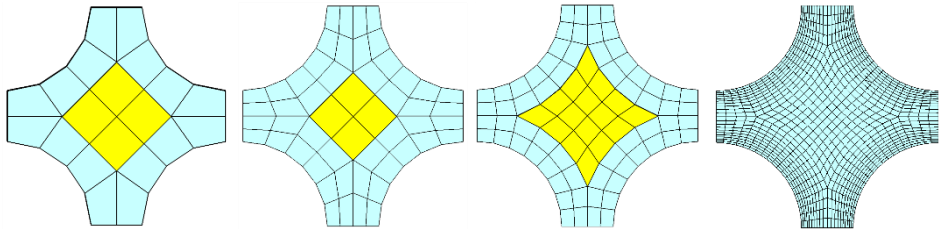

(a) Mesh-1 (b) Mesh-2 (c) Mesh-3 (d) CFD mesh

Figure 3: Comparison of the computing mesh set in SubChCFD and a RANS wall-function CFD mesh for a square-lattice PWR sub-channel

It can be seen clearly that the cell count in SubChCFD is much smaller than that in the conventional CFD mesh (in this case, only 20, 52 and 80 cells in Mesh-1, 2 and 3, while 624 cells in the CFD mesh). Accordingly, the computing cost is expected to be reduced by about 1 to 1.5 orders of magnitude in a 2-D case and 2 to 3 orders of magnitude in a full 3-D case, respectively. This is just a comparison with the wall-modelled CFD, the reduction in computing cost will be even more significant when compared with wall-resolved CFD simulations.

3 Application and Validation

In this study, the multi-purpose CFD package Code_Saturne developed by EDF R&D [60] is used as the platform to implement SubChCFD. Code_Saturne is a finite-volume method-based open-source software, providing the user full access to the source code. A well-defined user subroutine system allows the user to implement self-defined models and methods easily and conveniently. However, there is no reason why a method of this type could not be implemented in similar CFD codes.

3.1 Fully developed flow and heat transfer in a 5x5 PWR bundle

To demonstrate and validate the new methodology of SubChCFD in nuclear thermal-hydraulic modelling, a 2-D model is firstly created to simulate an axially fully developed flow in a rod bundle. The geometry of the bundle is taken from the OECD/NEA MATiS-H benchmarking experiment [61] in which the test section consists of a 5x5 rod bundle enclosed in a square housing. The geometrical features of the experimental rig are very similar to a real PWR fuel assembly, although the overall size is about three times bigger than the latter. Figure 4 shows some details of the cross-section of the rod bundle. The working fluid used in the experiment is water at a bulk temperature (T_0) of 35 ℃, an operating pressure of 1.5 bar, and a bulk velocity (u_0) of 1.5 m/s, corresponding to a Reynolds number ($Re_0 = \rho u_0 D_{h0}/\mu$) of 50,250. Although the Reynolds number is lower than a full size assembly under reactor conditions, this experimental test rig was specifically designed and used to generate high resolution velocity measurements for CFD model validation of turbulent mixing downstream of a PWR spacer grid. For such reason, it represents a good-quality test case for this study.

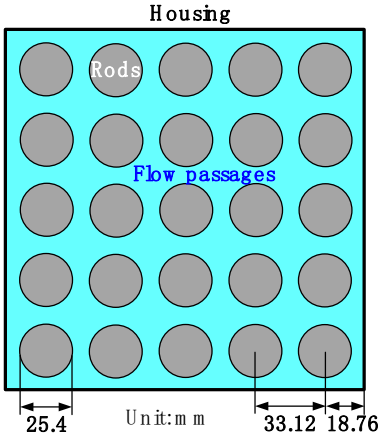

Figure 4: Sketch of the 5x5 rod bundle

In the original experiment, no heating was applied to the rods. In the simulation, a uniform 200 kW/m^2 heating is imposed to the surface of the rods to evaluate the performance of SubChCFD in heat transfer predictions. For the sake of simplicity, the density change due to temperature rise is assumed to be negligible so that the momentum transport is not coupled with heat transfer. In order to assist the validation process, a resolved CFD model that includes heat transfer, has also been created for the same geometry to provide reference results in addition to the experimental data. The computing mesh and the filtering mesh of the rod bundle used in SubChCFD are shown in Figure 5(a) and Figure 5(b), respectively. It should be noted that the computing mesh is generated based on Mesh-1 given in Figure 3. Figure 5(c) is the mesh used in the reference resolved CFD model. Since the flow inside the rod bundle is a wall-

bounded shear flow, the standard k-ε turbulence model and the scalable wall function are sufficient to produce reliable reference results.

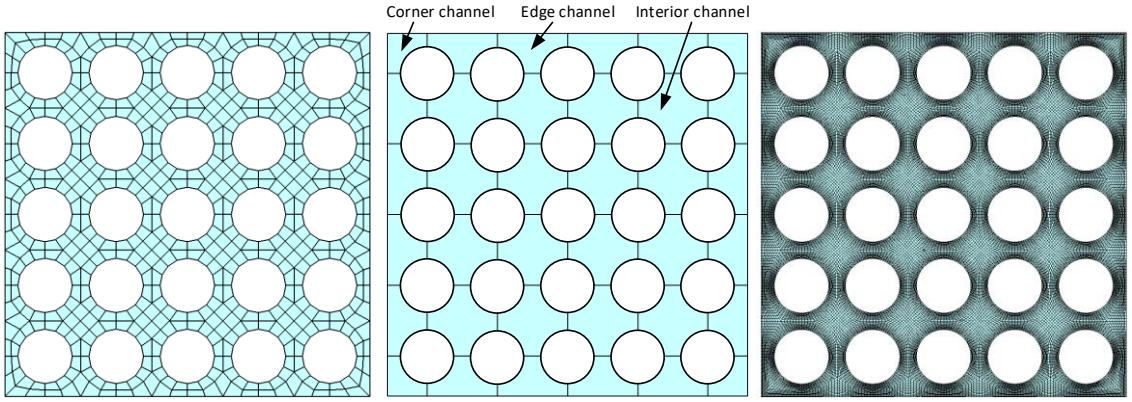

(a) (b) (c)

Figure 5: Meshes used in the simulation, including (a) SubChCFD computing mesh (560 cells), (b) SubChCFD filtering mesh, and (c) CFD mesh of the reference model (27,264 cells)

Since the flow studied here is axial and fully developed, periodic conditions are imposed on the boundaries perpendicular to the rods and only one layer of mesh is used in the stream-wise direction, which makes the model 2-D. Zero-gradient conditions are applied to all of the solid walls, whereas an empirical correlation of the frictional factor is used on the filtering mesh to calculate the wall friction which is further imposed as a momentum source term to the wall adjacent cells in the computational mesh to account for the wall shear effect. The frictional factor correlation used here is based on different types of sub-channels in a square-lattice rod bundle. It is given by the following expression [62],

$$f = \left[a + b_1 (P / D_h - 1) + b_2 (P / D_h - 1)^2 \right] / \mathrm{Re}^n \tag{6}$$

where P is the pitch of the rod array, D_h the sub-channel hydraulic diameter, Re the sub-channel Reynolds number. a, b_1, b_2 and n are model constants which can be found in **Error! Reference source not found.**.

Table 1: Parameters in the frictional factor correlation for square-lattice rod bundles [62]

Sub-channel type	a	b_1	b_2	n
Interior (laminar)	35.55	263.7	-190.2	1
Edge (laminar)	44.40	256.7	-267.6	1
Corner (laminar)	58.83	160.7	-203.5	1
Interior (turbulent)	0.1339	0.09059	-0.09926	0.18
Edge (turbulent)	0.143	0.04199	-0.04428	0.18
Corner (turbulent)	0.1452	0.02681	-0.03411	0.18

For the energy equation, a sink term is introduced to continuously remove a certain amount of heat which is in balance with that generated by the fuel rods so that a steady-state temperature field can be maintained. The energy sink is based on the computing mesh and can be calculated as follows,

$$S_E = -\frac{\Phi_{net}\vec{u}\cdot\vec{e}_z}{\int_{\Omega_d}\vec{u}\cdot\vec{e}_z dV} = -\frac{\Phi_{net}u_z}{\int_{\Omega_d}u_z dV} \tag{7}$$

where Φ_{net} is the net heat input to the fluid, $\vec{e}_z$ is the unit vector of the stream-wise direction, Ω_d represents the whole computational domain.

Since the wall heat flux has been directly given using a Neumann boundary condition, the Nusselt number correlation only plays a role to estimate the wall temperature when required. The situation is different when the SubChCFD energy equation is solved using Dirichlet boundary conditions, which are not used directly to close the discrete system, since the coarse mesh does not resolve the near-wall temperature field to ensure a correct wall heat flux calculated. Instead, the Nusselt number correlation is employed to convert the Dirichlet boundary condition into a Neumann boundary condition according to the following equation,

$$\dot{q} = -\frac{\lambda \cdot Nu}{D_h}\left(T_w^n - T_{sub}^{n-1}\right) \tag{8}$$

where the sub-channel bulk temperature T_{sub} is taken from the previous iteration.

The Nusselt number correlation used here for the rod bundle is derived as a product of $(Nu_\infty)_{c.t.}$ for the circular pipe in fully developed conditions multiplied with a correction factor [62].

$$Nu = \psi (Nu_\infty)_{c.t.} \tag{9}$$

where $\psi = 1 + 0.9120\,\mathrm{Re}^{-0.1}\,\mathrm{Pr}^{0.4}(1 - 2.0043e^{-B})$, $B=D_h/D$ (D is the rod diameter).

$(Nu_\infty)_{c.t.}$ is given by the Dittus-Boelter equation [63],

$$(Nu_\infty)_{c.t.} = \begin{cases} 0.023\,\mathrm{Re}^{0.8}\,\mathrm{Pr}^{0.4} & \text{when the fluid is heated} \\ 0.023\,\mathrm{Re}^{0.8}\,\mathrm{Pr}^{0.3} & \text{when the fluid is cooled} \end{cases} \tag{10}$$

Figure 6 shows the simulation results of the SubChCFD and resolved CFD for the 5x5 rod bundle. It can be seen that SubChCFD is capable of capturing the main features of the velocity and temperature fields in the sub-channels really well. It is also clear that SubChCFD does not show the stagnation and the hot spots close to the wall predicted by the resolved CFD as expected by the nature of this approach. Figure 7 provides a more detailed comparison using line plots, in which experimental data are also provided where available. It is first noted that the resolved CFD seems to overpredict the velocity variation between the rod bundles measured in the experiment. The results of the SubChCFD model follow the resolved CFD results closely and also over-predict the temperature variations. Consequently, both models can successfully capture the overall trend of the flow pattern and both of them have similar deviations from the experimental measurements (in both cases the modelling methods would not be expected to capture any anisotropy of the flow).

In order to evaluate the mesh-dependency of SubChCFD, two other computing meshes, based on resolutions of Mesh-2 and Mesh-3 respectively, are used to simulate the flow in the 5x5 rod bundle under the same flow conditions. The results are shown in Figure 8 and compared with the Mesh-1 result. It is interesting to observe that the results are nearly mesh independent, e.g. the three meshes produce very similar results in terms of both velocity and temperature fields. This suggests that numerical diffusion plays a relatively small role for this type of wall-bounded shear flow. However, it is worth noting that the Mesh-1 result deviates from the other two meshes in some regions of the edge sub-channel and the corner sub-channel.

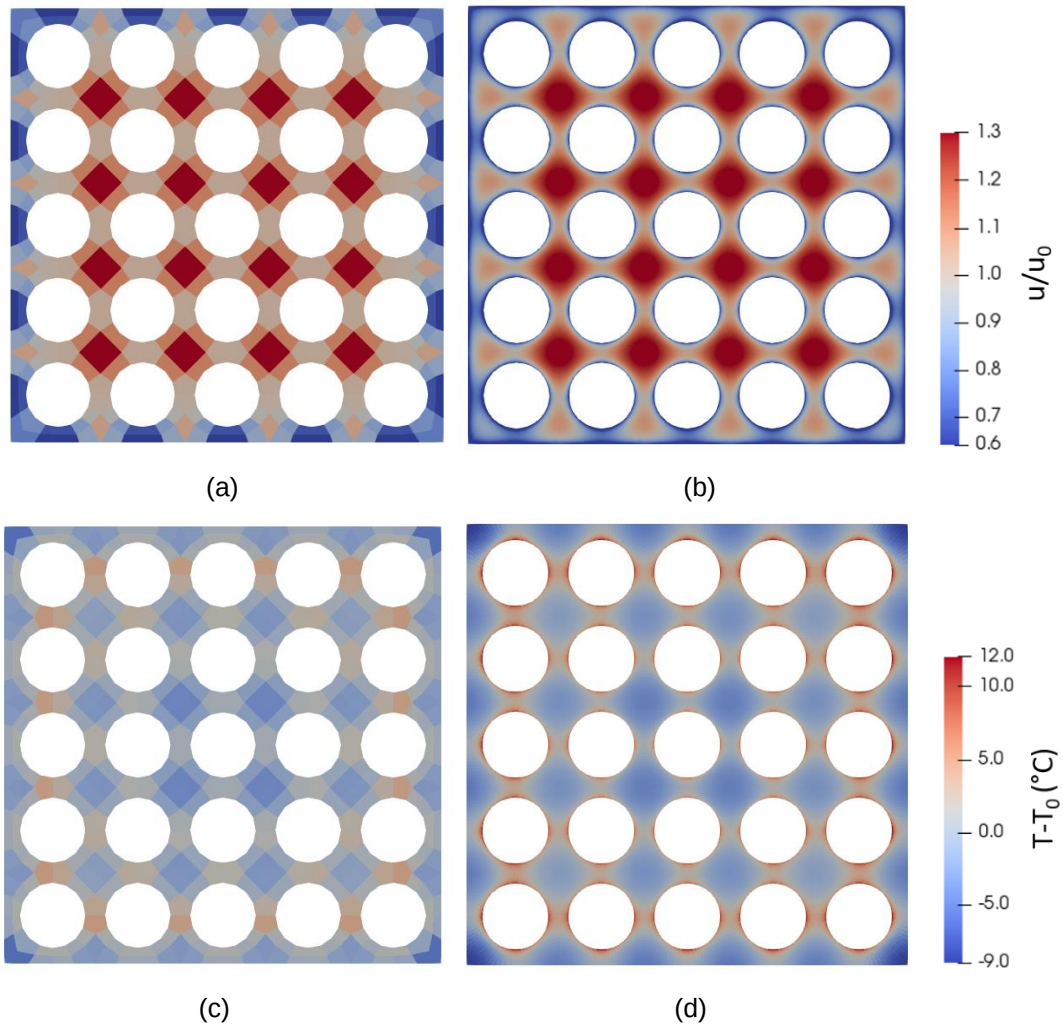

Figure 6: Contour plots of the 5x5 bundle, (a) and (b) the normalized axial velocity distribution derived from SubChCFD and resolved CFD simulations, (c) and (d) the temperature distribution derived from SubChCFD and resolved CFD simulations

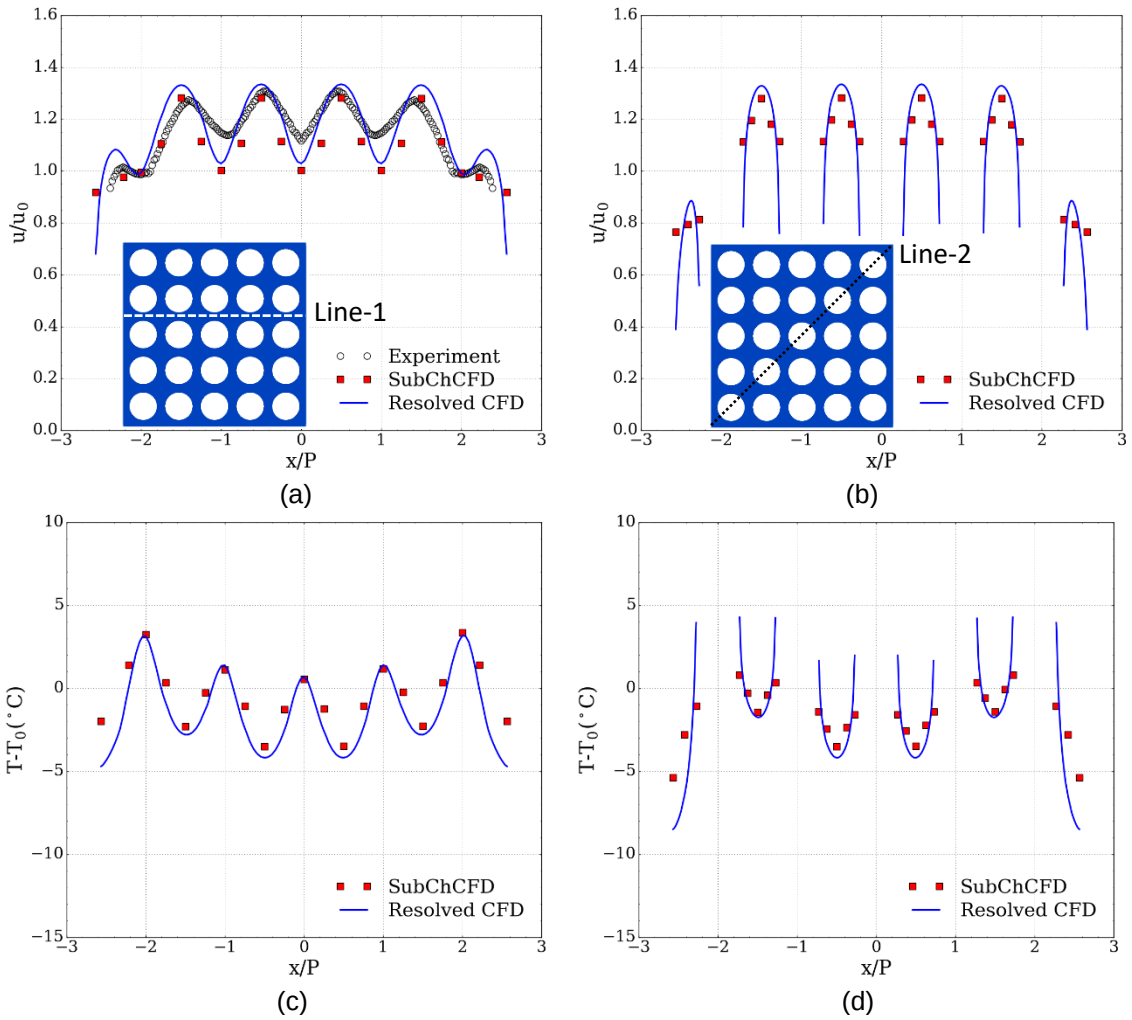

Figure 7: Line plots of the 5x5 bundle, (a) and (b) the normalized axial velocity over Line-1 and Line-2, (c) and (d) temperature over Line-1 and Line-2

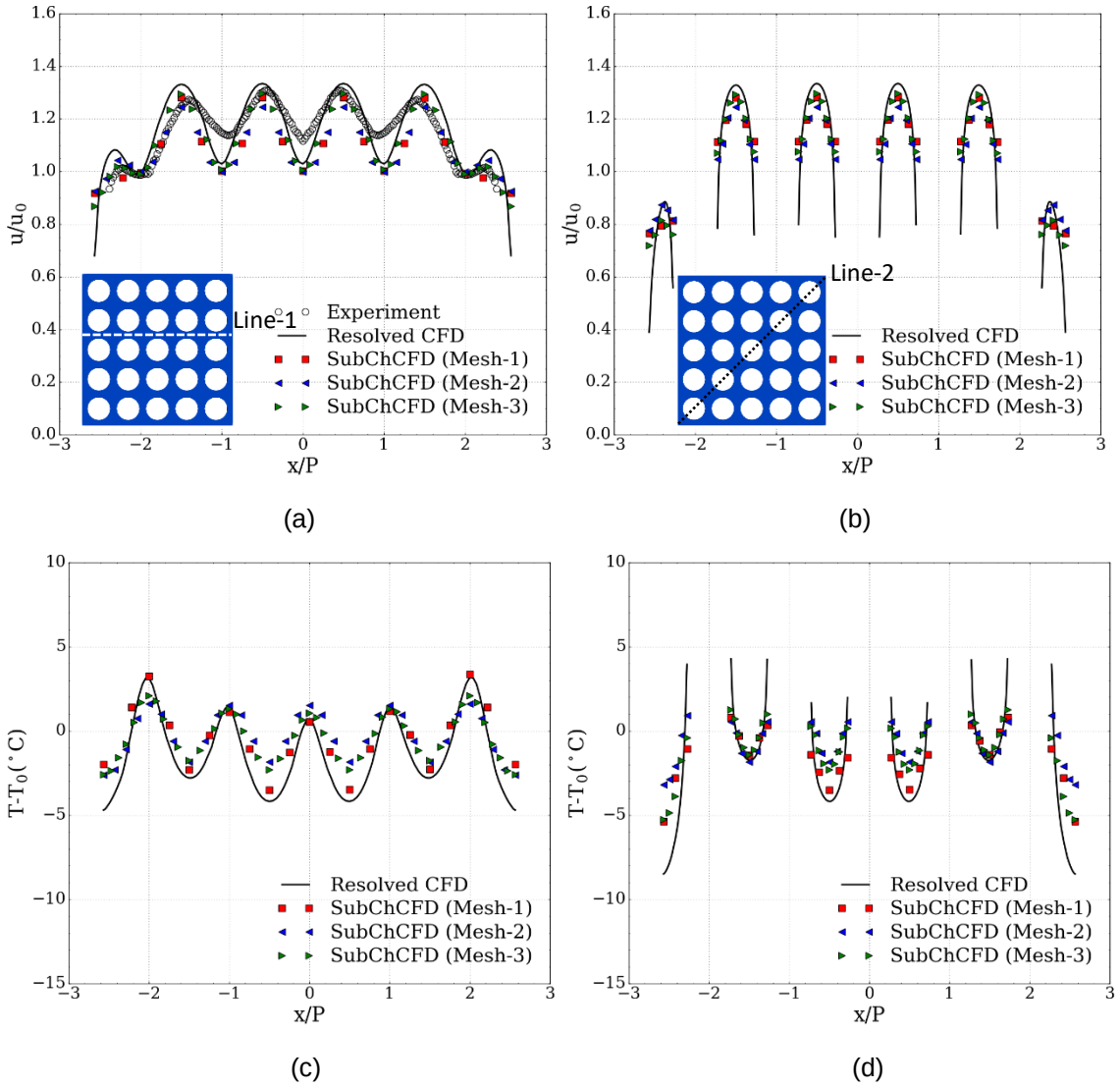

Figure 8: Mesh-dependency test, (a) and (b) the normalized axial velocity over Line-1 and Line-2, (c) and (d) temperature over Line-1 and Line-2

To further assess the performance of SubChCFD, simulations have been carried out for two additional cases derived by altering the distribution of the heating source and the geometrical layout of the rods of the base-line validation case.

The first case is aimed at testing the performance of SubChCFD when applied to non-uniformly heated bundles. This occurs in reactors, for example, following refuelling when fresh fuel sits next to the boundary of a partially spent fuel assembly. For the sake of simplicity, a non-uniform thermal environment is created in this test case by imposing a 200 kW/m^2 heat loading to the centre rod with all other rods being adiabatic. Figure 9 and Figure 10 show the resulting temperature field predictions. It can be seen that the temperature distribution predicted by SubChCFD agrees well with that exhibited in the results of the resolved CFD in this non-uniform heating scenario.

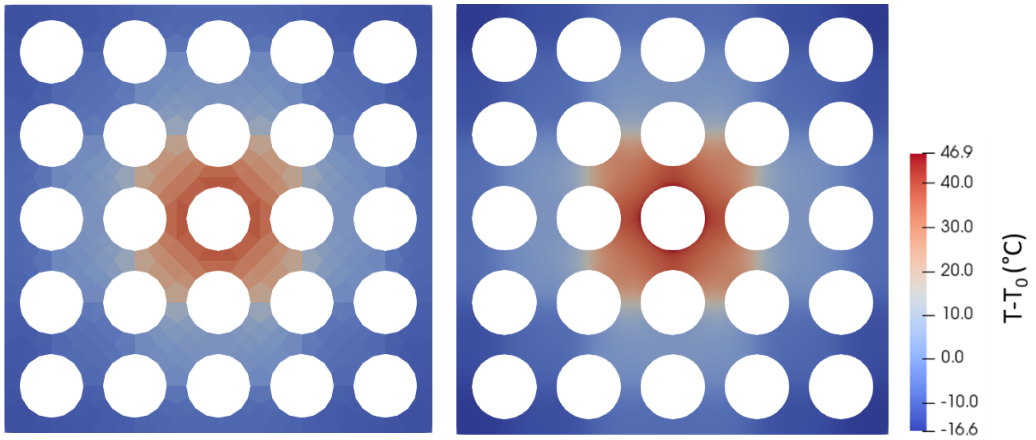

Figure 9: Temperature distribution of non-uniformly heated bundle obtained with (a) SubChCFD and (b) resolved CFD

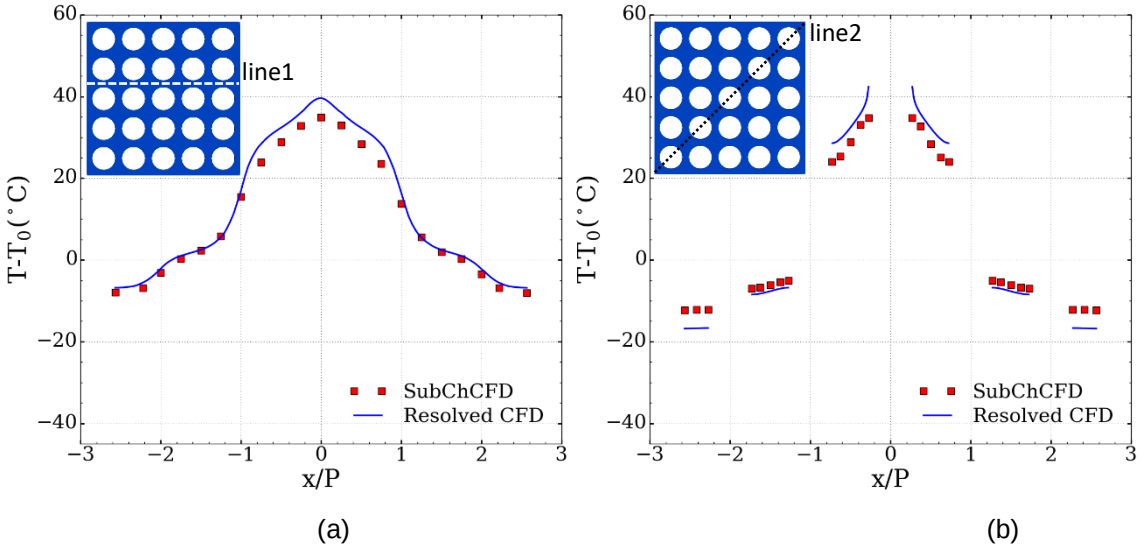

Figure 10: Line plots of the temperature field over (a) Line-1 and (b) Line-2

The second case is aimed at testing SubChCFD for geometrically distorted rod bundles, which is also of great importance in engineering practice, especially for safety assessment. Here, one column of the rods is shifted slightly to one side, creating a widened and a narrowed sub-channel on the two sides, respectively. The gap width is increased by 1.5 times in the former and is halved in the latter compared with a regular channel. The geometry change is expected to redistribute the mass flow among the sub-channels, leading to significant non-uniformity of the temperature distribution. Figure 11 and Figure 12 show the simulation results of SubChCFD and the resolved CFD for the distorted rod bundle. It can be seen that SubChCFD responds to the geometrical change very well in terms of flow redistribution. The temperature redistribution has also been qualitatively captured, for example, the local increase in temperature caused by the reduction of the coolant flow in narrow sub-channels, although the agreement could be further improved if required by calibrating some of the model parameters, such as the turbulent Prandtl number.

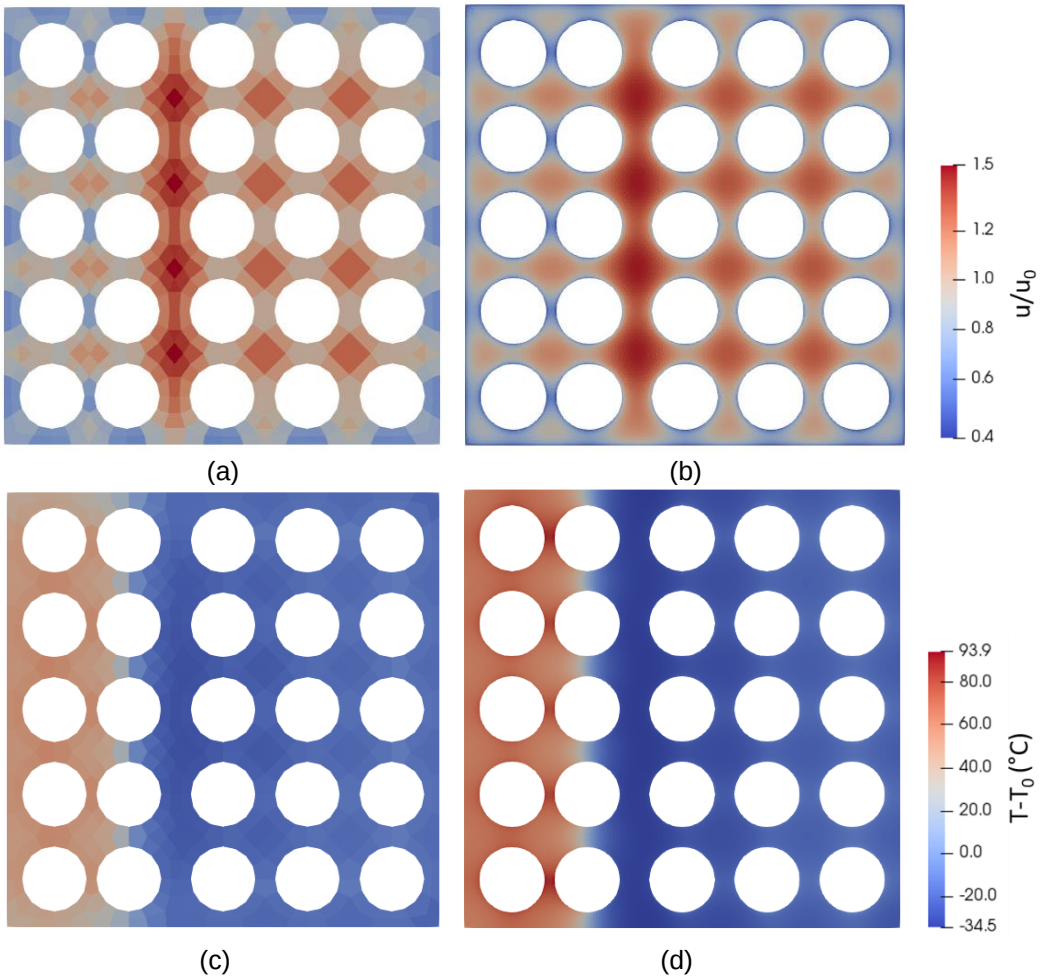

Figure 11: Simulation results of the geometrically altered rod bundle, (a) and (b) the normalized axial velocity fields, (c) and (d) the temperature fields

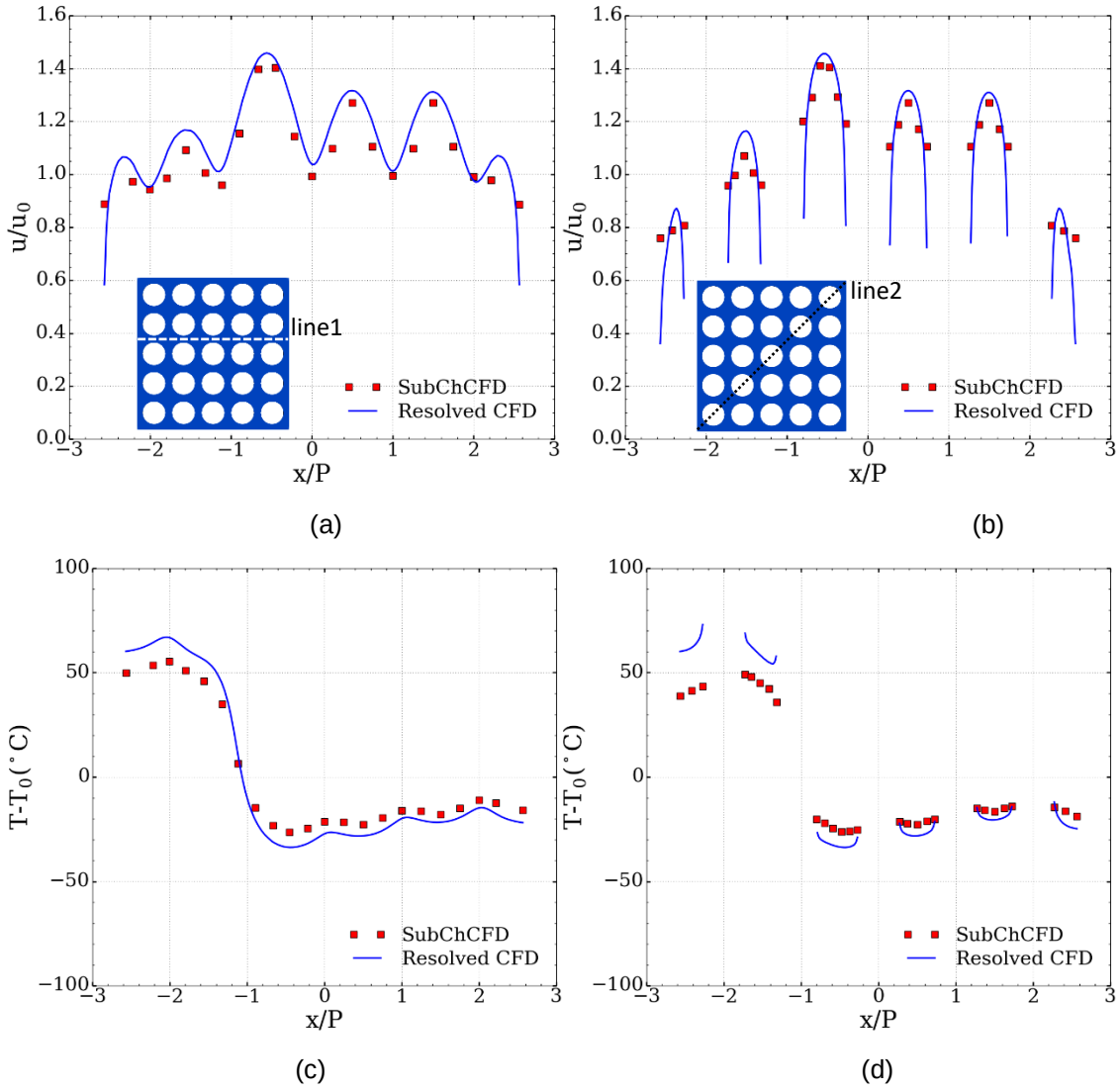

Figure 12: Line plots of the velocity and temperature fields, (a) and (b) normalized axial velocity over Line-1 and Line-2, (c) and (d) normalized temperature over Line-1 and Line-2

The above test cases have demonstrated the feasibility of SubChCFD for calculations of fuel bundle flow and heat transfer. It is not only able to predict sub-channel-level behaviours but also to capture sub-scale physics within the sub-channels. Benefiting from the greatly reduced computing cost compared to resolved CFD, SubChCFD can be used for simulation of large-scale reactor components. In the following sections, the performance of SubChCFD for full 3-D large-scale bundle flows is assessed further.

3.2 Flow and heat transfer in a partially blocked 5x5 PWR bundle

The following case is used to test the capability of SubChCFD in tackling non-design operating circumstances. It is created by positioning a blockage in one of the sub-channels to obstruct the flow at a certain height in a 5x5 rod bundle. Geometrical details of the obstruction can be found in Figure 13(a) and Figure 13(b). During operations in nuclear reactors, partial or complete

blocking of single or multiple sub-channels of the reactor core is considered to be a credible scenario, for example, in PWR reactors due to LOCA-related rod swelling or ballooning [64].

Due to the local blockage, the nearby coolant flow is significantly distorted, resulting in locally strengthened inter-channel mixing and lateral flow. The traditional sub-channel codes would find this a very challenging problem to calculate due to the restrictions of the 1-D framework of formulation used. Some special treatment might be developed but it is impossible for such an approach to describe the 3-D flow phenomenon around the blockage and the large scale recirculation downstream in any detail. In contrast, SubChCFD is naturally applicable. Figure 13(c) shows the extruded mesh of a cross-section passing through the blockage region, which is generated based on the resolution of computing Mesh-2. The total number of mesh cells for the entire 3-D SubChCFD model is about 0.645 million. This is much lower than that used in the CFD reference model which consists of 21 million hexahedral mesh cells.

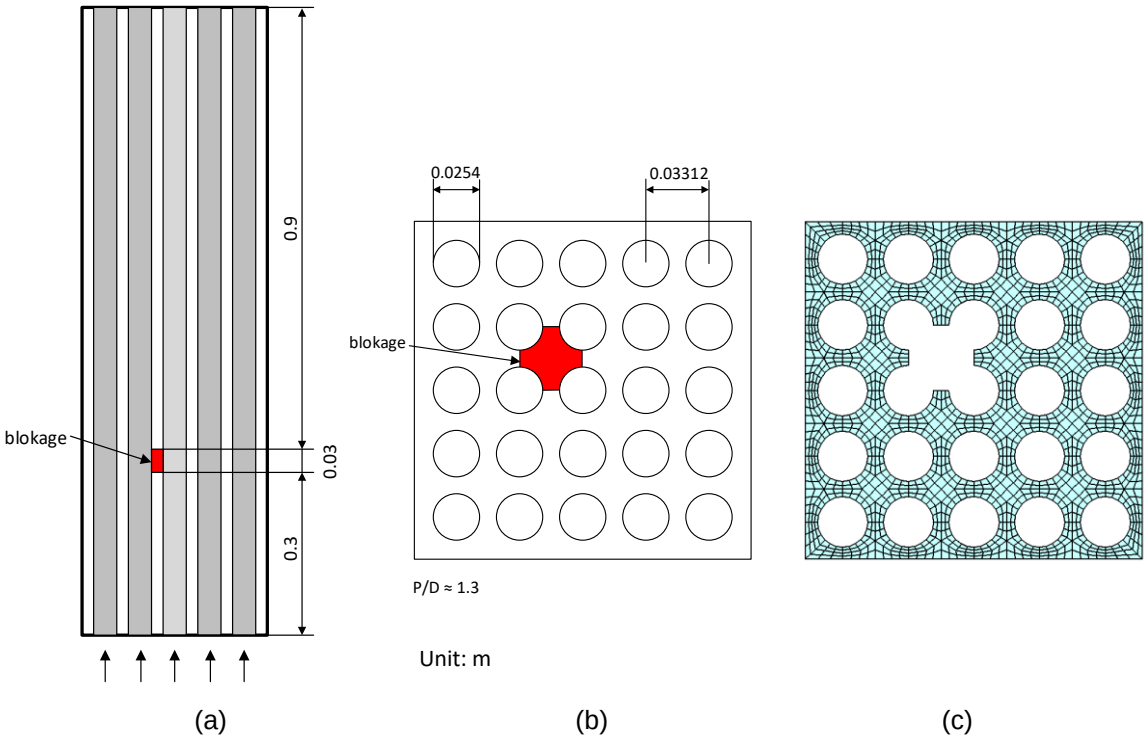

Figure 13: Geometry and mesh of the 3-D rod bundle with local blockage, (a) and (b) the longitudinal and the cross-section view of the rod bundle (unit in m), (c) a cross-section of the computing mesh used in the SubChCFD model

Figure 14 shows comparisons between the simulation results produced using SubChCFD and the resolved CFD. The x-component of the cross-flow velocity is firstly plotted along a horizontal line (i.e. Line-1 in Figure 14(a)), which reflects the profile of the lateral flow distribution around the blockage area. It can be seen that SubChCFD produces a very similar result to that of the resolved CFD. In this region, the Bernoulli's effect plays a leading role in shaping the local flow around the blockage, which can be captured by SubChCFD. However, there are pressure losses due to re-circulation around the blockage, which are not currently modelled in SubChCFD. This does not affect the results significantly here, but the pressure losses could be accounted for in the model in the future.

Figure 14(c) shows the pressure distribution along Line-2 shown in Figure 14(a). As can be seen from the figures, the overall trend of the pressure variation is captured but some details,

such as the appearance of the lower peak, cannot be reproduced with the SubChCFD simulations.

Figure 14(d) shows the axial pressure distribution along the centre line of sub-channel A (the sub-channel on the right-hand side close to the blockage, see Figure 14(a)). It is worth noting that SubChCFD agrees very well with the resolved CFD in predicting the frictional loss of the non-blocked section and form loss of the blocked section, even though the local peak value is not accurately captured in terms of comparison to the resolved simulation results. The sharp pressure dips are linked to the rapid local flow acceleration due to the reduced area. This is an inviscid effect and so the pressure recovers and the velocity returns to its original value past the restricted flow area region, which explains why SubChCFD does not reproduce this effect accurately, i.e. this sharp change, does not affect its overall performance.

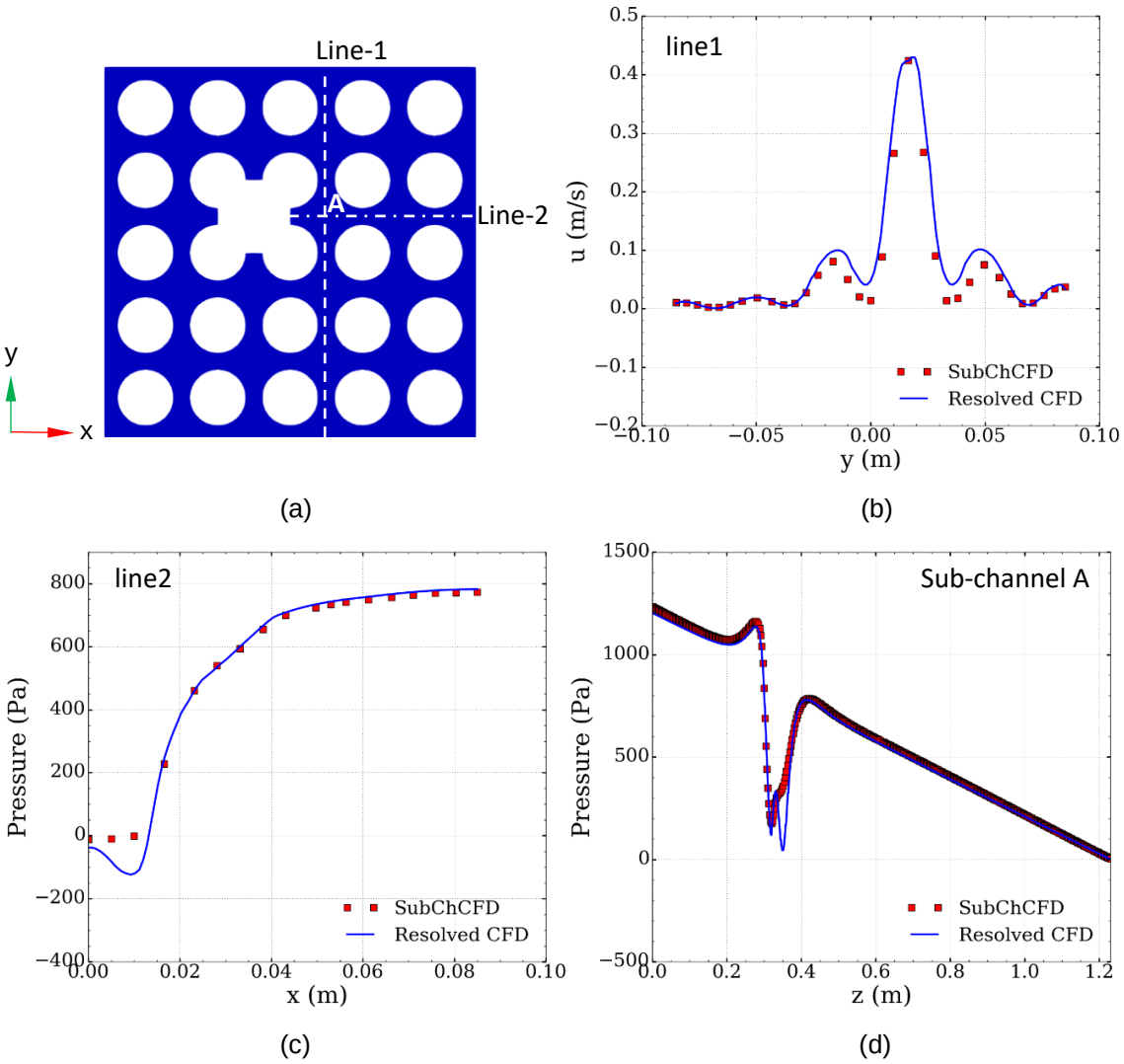

Figure 14: Simulation results of the 3-D bundle with local blockage, (a) position of lines for plotting, (b) velocity in x-direction alone Line-1, (c) transverse pressure distribution alone Line-2, (d) axial pressure loss in Sub-channel A

3.3 Flow in a partially blocked 14x14 parallel assembly

The experimental test of flow in a 14x14 parallel fuel assembly was carried out by Weiss et al. [65], aimed at investigating the flow redistribution between two open fuel assemblies resulting from a partial or full blockage at the entrance of one assembly. This case has also been studied numerically by S.J. Yoon et al. [66] using their newly developed sub-channel code CUPID. This is a perfect case for direct comparison between SubChCFD and the sub-channel codes used in large-scale component modelling.

The test section of the experimental rig consists of two 14x14 fuel assemblies interconnected through a water gap and enclosed in a rectangular housing (see Figure 15). Each of the assemblies is 0.1869 m in width and 0.1938 m in height, and the width of the water gap is 0.0155 m. The diameter of the rods is 0.0108 m and the pitch-to-diameter ratio is 1.28. The fuel assembly on the right-hand side is assumed to be partially blocked at the entrance, resulting in a reduced mass flux compared to the left assembly. In the numerical simulation, to reproduce the mass flow rates of 550 g/min and 1,110 g/min for the two bundles, inlet bulk velocities are set to 1.76 m/s and 3.52 m/s, respectively. For the water gap, the inlet velocity is given an average value of 2.64 m/s.

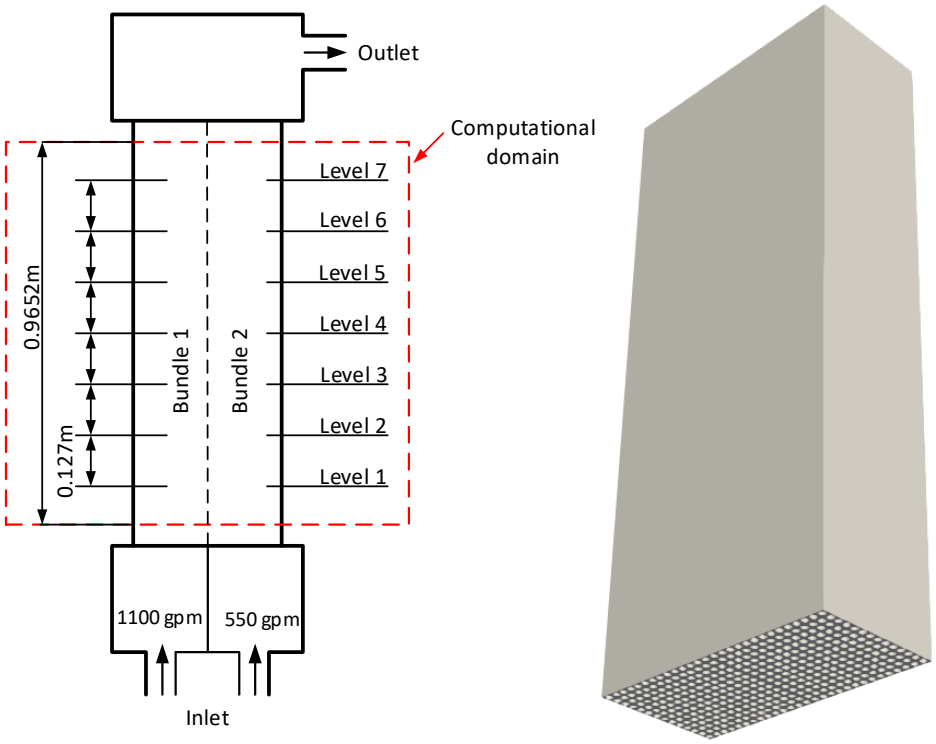

Figure 15: Modelling of the parallel fuel assembly, (a) schematic of the experimental facility, (b) numerical model of the test section

Figure 16 shows the cross-section view of the computing mesh used for the parallel fuel assembly based on the resolution of Mesh-1. As can be seen from the zoomed-in inset, the distribution of the grid lines has been adjusted slightly in the edge sub-channels to improve the quality of the mesh elements close to the wall. Based on this resolution, 3.3 million hexahedral mesh elements were generated for the entire 3-D SubChCFD computing mesh. A resolved CFD simulation for this case would need about 400 million cells, which is a large model even for current Tier-1/Tier-2 HPC research facilities.

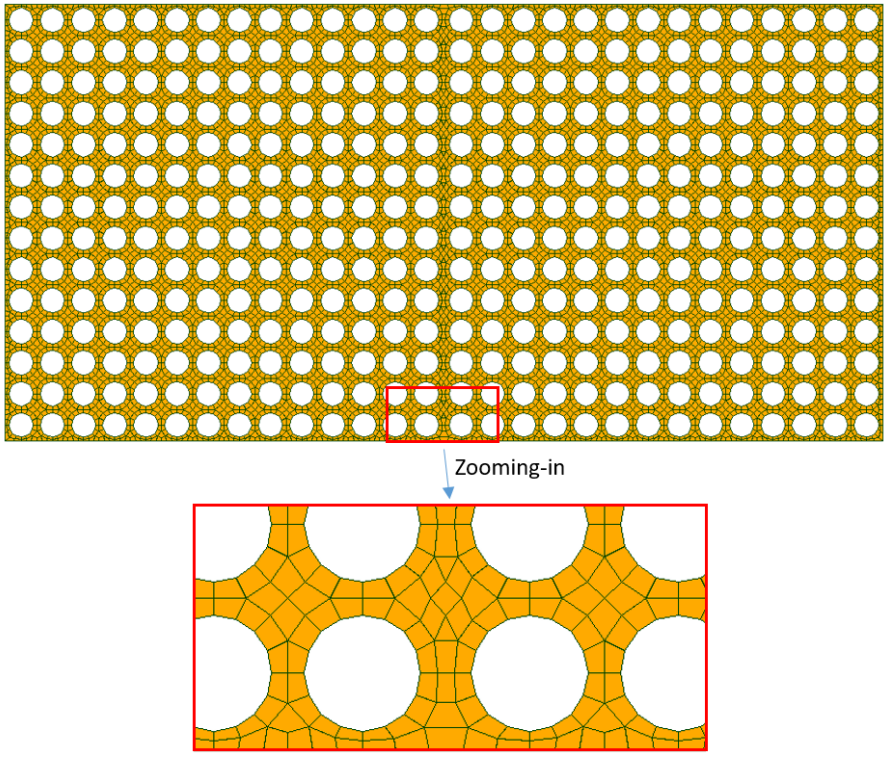

Figure 16: Cross-section view of the computing mesh for the parallel assembly

Instead of conducting a resolved CFD simulation, the results of the SubChCFD were evaluated by comparing them with those obtained from the sub-channel code CUPID and the available experimental data. Figure 17 shows the axial velocity profiles at six different vertical elevations of the parallel assembly. They are plotted using mean values calculated by arithmetic averaging at three sampling locations in accordance with the experimental measuring points, located at the centre lines between Row-2 and Row-3, Row-7 and Row-8, and Row-12 and Row-13 of the fuel rods, respectively.

For most of the levels (except Level 2), the SubChCFD results agree somewhat better with the experimental data than those produced by CUPID. Moreover, as expected, SubChCFD provides more details of the flow profile than the traditional sub-channel code. For instance, the variation of the axial velocity occurring between the gap and the centre of the sub-channel are well captured. These variations appear to be smaller nearer the mixing interface as expected, where the strong cross flow and mixing smooth out the velocity gradients. Such phenomena cannot be predicted using a traditional sub-channel code.

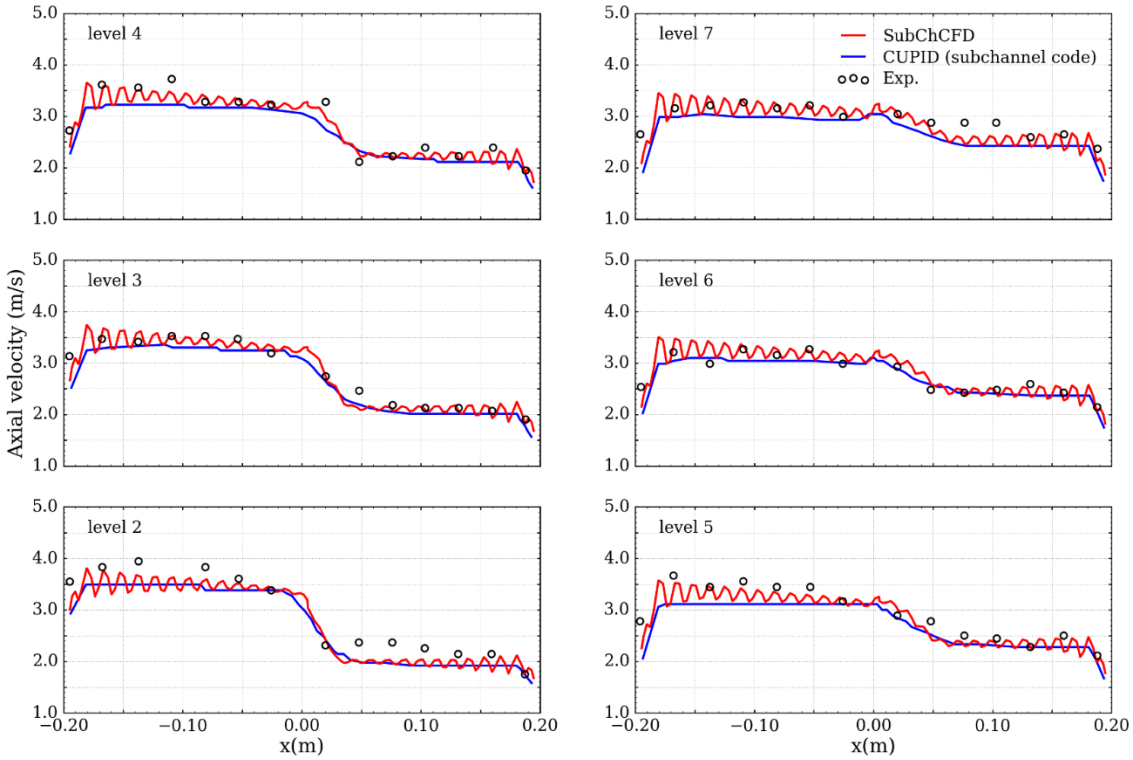

Figure 17: Axial mean velocity profiles of the parallel assembly

4 Conclusions

A coarse-grid CFD-based modern sub-channel methodology (SubChCFD) has been developed to fill the gap between the system/sub-channel codes and conventional CFD. The convection term is directly discretised on the coarse mesh and the diffusion term is split into two parts, including the near-wall and non-near-wall parts, respectively. The latter is then described using a 0-equation mixing length turbulence model, whilst the former is tackled in a similar way as that normally done in a sub-channel analysis code, using empirical correlations as closure laws. In doing so, on one hand, the computing cost is significantly reduced compared to conventional CFD methods due to the use of a coarse mesh, making it possible to simulate large reactor components or even the whole core. On the other hand, some advanced features from conventional CFD can be retained, such as full 3-D results, high simulation robustness and application flexibility, etc.

The methodology of SubChCFD has been implemented into the open-source CFD package Code_Saturne. A numerical test has been done for the 5x5 bare rod bundle of the OECD/NEA MATiS-H benchmarking experiment. This shows that SubChCFD demonstrates good numerical stability and robustness, and is able to capture the flow and heat transfer well in this axially dominant bundle flow, with a significant reduction in computing cost compared to conventional CFD.

SubChCFD has also been used to simulate two complex 3-D flow cases. The first case is a locally blocked rod bundle derived by placing an obstruction in one of the sub-channels. The cross-flow due to the blockage has been well captured and the predicted axial pressure loss due to friction and obstruction are in good agreement with those obtained in resolved CFD simulations. The second case comprises two parallel fuel assemblies with different input mass flow rate. In this case, SubChCFD also produces excellent predictions, not only by successfully capturing the distribution of the axial velocity due to the inter-channel mixing but also by providing flow details within sub-channels which cannot be captured by the traditional sub-channel codes.

In the future, SubChCFD will be further developed to broaden the scope of its application, including, for example, transverse-dominant flows, buoyancy-influenced mixed convection or natural circulation. Coupling with resolved CFD and/or a porous media method will also be explored.

5 References

1. Moorthi, A. Kumar Sharma, & K. Velusamy, A review of sub-channel thermal hydraulic codes for nuclear reactor core and future directions. Nuclear Engineering and Design, 332 (2018) 329–344.

2. W. T. Sha, An overview on rod-bundle thermal-hydraulic analysis. Nuclear Engineering and Design, 62 (1980) 1–24.

3. G. Yadigaroglu, M. Andreani, J. Dreier, & P. Coddington, Trends and needs in experimentation and numerical simulation for LWR safety. Nuclear Engineering and Design, 221 (2003) 205–223.

4. RELAP5 Development Team, RELAP5/MOD3 Code Manual Code Structure, System Models, and Solution Methods. (1995) Idaho National Engineering Laboratory.

5. G. Lerchl, H. Austregesilo, H. Glaeser, M. Hrubisko, & W. Luther, ATHLET MOD3.0 Cycle A. (2012).

6. D. Bestion, The physical closure laws in the CATHARE code. Nuclear Engineering and Design, 124 (1990) 229–245.

7. D. R. Liles & J. H. Mahaffy, TRAC-PF1/MOD1: An Advanced Best-estimate Computer Program for Pressurized Water Reactor Thermal-hydraulic Analysis. NUREG/CR-3858, (1986) Los Alamos National Laboratory.

8. D. S. Rowe, Cross-flow mixing between parallel flow channels during boiling part I COBRA - computer program for coolant boling in rod arrays. Review Literature And Arts Of The Americas, (1967) No. BNWL-371 (Pt. 1). Battelle-Northwest, Richland.

9. C. W. Stewart, J. M. Cuta, A. S. Koontz, J. M. Kelly, K. L. Basehore, T. L. George, & D. S. Rowe, VIPRE-01: A Thermal-Hydraulic Analysis Code for Reactor Cores Volume 1. Mathmatical Modeling. [PWR; BWR]. (1983) No. EPRI-NP-2511-CCM-Vol. 1. Battelle Pacific Nort.

10. D. H. Hwang, K. W. Seo, & H. Kwon, Validation of a Subchannel Analysis Code MATRA Version 1.0. (2008) No. KAERI/TR--3639/2008. Korea Atomic Energy Resea.

11. L. Brockmeyer, L. B. Carasik, E. Merzari, & Y. A. Hassan, CFD Investigation of Wire-Wrapped Fuel Rod Bundle Inner Subchannel Behavior and Dependency on Bundle Size. Proceedings of the 24th International Conference on Nuclear Engineering - ICONE 24, (2016) 1–9.

12. H.-Y. Jeong, K.-S. Ha, W.-P. Chang, Y.-M. Kwon, & Y.-B. Lee, Modeling of Flow Blockage in a Liquid Metal-Cooled Reactor Subassembly with a Subchannel Analysis Code. Nuclear Technology, 149 (2005) 71–87.

13. F. Yu, A. Class, J. Xiao, & T. Jordan, Coarse grid CFD methodology: flux corrections for individual mesh cells and application to rod bundles. Proc. 17th Int. Top. Meet. Nucl. React. Therm. (Xi'an, 2017).

14. X. Z. Cui & K. Y. Kim, Three-dimensional analysis of turbulent heat transfer and flow through mixing vane in a subchannel of nuclear reactor. Journal of Nuclear Science and Technology, 40 (2003) 719–724.

15. G. Házi, On turbulence models for rod bundle flow computations. Annals of Nuclear Energy, 32 (2005) 755–761.

16. M. Imaizumi, T. Ichioka, M. Hoshi, H. Teshima, H. Kobayashi, & T. Yokoyama, Development of CFD method to evaluate 3-D flow characteristics for PWR fuel assembly. Trans. 13th Int. Conf. Struct. Mech. React. Technol. (Porto Alegre, 1995), pp. 1–12.

17. Z. Karouta, C.-Y. GU, & B. Schoelin, 3-D flow analyses for design of nuclear fuel spacer. Proc. 7th Int. Meet. Nucl. React. Therm. (New York, 1995).

18. G. Chen, Z. Zhang, Z. Tian, L. Li, X. Dong, & H. Ju, Design of a CFD scheme using multiple RANS models for PWR. Annals of Nuclear Energy, 102 (2017) 349–358.

19. B. Han, B. Wang, Z. Zhou, & Y. Zha, Numerical study on the effect of grid mixing span in 2×1 spacer grid. Proc. 17th Int. Top. Meet. Nucl. React. Therm. (Xi'an, 2017).

20. C. C. Liu & Y. M. Ferng, Numerically simulating the thermal-hydraulic characteristics within the fuel rod bundle using CFD methodology. Nuclear Engineering and Design, 240 (2010) 3078–3086.

21. C. C. Liu, Y. M. Ferng, & C. K. Shih, CFD evaluation of turbulence models for flow simulation of the fuel rod bundle with a spacer assembly. Applied Thermal Engineering, 40 (2012) 389–396.

22. Y. S. Tseng, Y. M. Ferng, & C. H. Lin, Investigating flow and heat transfer characteristics in a fuel bundle with split-vane pair grids by CFD methodology. Annals of Nuclear Energy, 64 (2014) 93–99.

23. H. Zhao, B. Yang, & Y. Zha, Analysis of the Three Dimension Flow Field of Single and Multi-Span Fuel Assemblies. Proc. 17th Int. Top. Meet. Nucl. React. Therm. (Xi'an, 2017).

24. V. Y. Agbodemegbe, X. Cheng, E. H. K. Akaho, & F. K. A. Allotey, An investigation of the effect of split-type mixing vane on extent of crossflow between subchannels through the fuel rod gaps. Annals of Nuclear Energy, 88 (2016) 174–185.

25. A. Ala, S. Tan, A. Eltayeb, M. Zhengpeng, & L. Xing, Simulation Study of Turbulent Flow Through 5x5 Rod Bundle. Proc. 17th Int. Top. Meet. Nucl. React. Therm. (Xi'an, 2017).

26. U. Bieder, Analysis of the IAEA-benchmark on flow mixing in a 4x4 rod bundle. Proc. 17th Int. Top. Meet. Nucl. React. Therm. (Xi'an, 2017).

27. U. Bieder, F. Falk, & G. Fauchet, LES analysis of the flow in a simplified PWR assembly with mixing grid. Progress in Nuclear Energy, 75 (2014) 15–24.

28. R. Denefle, M. C. Gauffre, & S. Benhamadouche, CFD Study of Flow Redistributions in PWR Fuel Assemblies. Proc. 17th Int. Top. Meet. Nucl. React. Therm. (Xi'an, 2017).

29. K. Ikeda, CFD application to advanced design for high efficiency spacer grid. Nuclear Engineering and Design, 279 (2014) 73–82.

30. S. K. Kang & Y. A. Hassan, Computational fluid dynamics (CFD) round robin benchmark for a pressurized water reactor (PWR) rod bundle. Nuclear Engineering and Design, 301 (2016) 204–231.

31. N. Tsuji, M. Nakano, E. Takada, K. Tokuhara, K. Ohashi, F. Okamoto, Y. Tazawa, Y. Inaba, & Y. Tachibana, Study of the applicability of CFD calculation for HTTR reactor. Nuclear Engineering and Design, 271 (2014) 564–568.

32. K. Takamatsu, Thermal-hydraulic analyses of the High-Temperature engineering Test Reactor for loss of forced cooling at 30% reactor power. Annals of Nuclear Energy, 106 (2017) 71–83.

33. J. P. Simoneau, J. Champigny, B. Mays, & L. Lommers, Three-dimensional simulation of the coupled convective, conductive, and radiative heat transfer during decay heat removal in an HTR. Nuclear Engineering and Design, 237 (2007) 1923–1937.

34. M. Kao, C. Wu, C. Chieng, Y. Xu, K. Yuan, M. B. Dzodzo, M. E. Conner, S. Beltz, S. Ray, & T. Bissett, CFD Analysis of PWR Reactor Vessel Upper Plenum Sections- Flow Simulation in Control Rods Guide Tubes. Proc. 18th Int. Conf. Nucl. Eng. (Xi'an, 2010), pp. 1–8.

35. M. T. Kao, C. Y. Wu, C. C. Chieng, Y. Xu, K. Yuan, M. Dzodzo, M. Conner, S. Beltz, S. Ray, & T. Bissett, CFD analysis of PWR core top and reactor vessel upper plenum internal subdomain models. Nuclear Engineering and Design, 241 (2011) 4181–4193.

36. K. Podila, Y.F. Rao, M. Krause, & J. Bailey, A CFD simulation of 5X5 rod bundles with split-type spacers. Progress in Nuclear Energy, 70 (2014) 167-175.

37. Kazuo Ikeda, CFD application to advanced design for high efficiency spacer grid. Nuclear Engineering and Design, 279 (2014) 73–82.

38. S. Benhanmadouche, P. Moussou, & C. Le Maitre, CFD estimation of the flow-induced vibrations of a fuel rod downstream a mixing grid. Proc. ASME 2009 Press. Vessel. Pip. Div. Conf. (Prague, Czech Republic, 2009), pp. 1–9.

39. Shams, F. Roelofs, E. M. J. Komen, & E. Baglietto, Quasi-direct numerical simulation of a pebble bed configuration. Part I: Flow (velocity) field analysis. Nuclear Engineering and Design, 263 (2013) 473–489.

40. P. Fischer, J. Lottes, A. Siegel, & G. Palmiotti, Large eddy simulation of wire-wrapped fuel pins I: Hydrodynamics in a Periodic Array. Jt. Int. Top. onMathematics Comput. Supercomput. Nucl. Appl. (M&C + SNA 2007) (Monterey, California, 2007).

41. T. P. Grunloh & A. Manera, A novel domain overlapping strategy for the multiscale coupling of CFD with 1D system codes with applications to transient flows. Annals of Nuclear Energy, 90 (2016) 422–432.

42. N. Anderson, Y. Hassan, & R. Schultz, Analysis of the hot gas flow in the outlet plenum of the very high temperature reactor using coupled RELAP5-3D system code and a CFD code. Nuclear Engineering and Design, 238 (2008) 274–279.

43. Papukchiev, G. Lerchl, J. Weis, M. Scheuerer, & H. Austregesilo, Development of a coupled 1D-3D Thermal-Hydraulic Code for Nuclear Power Plant Simulation and its Application to a

Pressurized Thermal Shock Scenario in PWR. Proc. 14th Int. Top. Meet. Nucl. React. Therm. Conf. (Toronto, 2011).

44. T. Bury, Coupling of CFD and lumped parameter codes for thermal-hydraulic simulations of reactor containment. Computer Assisted Methods in Engineering and Science, 20 (2013) 195–206.

45. R. Bavière, N. Tauveron, F. Perdu, E. Garré, & S. Li, A first system/CFD coupled simulation of a complete nuclear reactor transient using CATHARE2 and TRIO-U. Preliminary validation on the Phénnix reactor natural circulation test. Nuclear Engineering and Design, 277 (2014) 124–137.

46. Z. Chen, X. N. Chen, A. Rineiski, P. Zhao, & H. Chen, Coupling a CFD code with neutron kinetics and pin thermal models for nuclear reactor safety analyses. Annals of Nuclear Energy, 83 (2015) 41–49.

47. Fiorina, I. Clifford, M. Aufiero, & K. Mikityuk, GeN-Foam: A novel OpenFOAM® based multi-physics solver for 2D/3D transient analysis of nuclear reactors. Nuclear Engineering and Design, 294 (2015) 24–37.

48. P. Skibin, V. Y. Volkov, L. A. Golibrodo, A. A. Krutikov, O. V Kudryavtsev, Y. N. Nadinskiy, & O. K. B. Gidropress, Development of CFD-Model of AES-2006 Reactor. Proc. 17th Int. Top. Meet. Nucl. React. Therm. (Xi'an, 2017).

49. Y. Yu, E. Merzari, A. Obabko, & J. Thomas, A porous medium model for predicting the duct wall temperature of sodium fast reactor fuel assembly. Nuclear Engineering and Design, 295 (2015) 48–58.

50. R. A. Brewster, T. A. Bissett, & Y. Xu, Computational Fluid Dynamics Assessment of Baffle Plate Leakage Flow Effects in a Downflow 4-Loop Reactor. Proc. 17th Int. Top. Meet. Nucl. React. Therm. (Xi'an, 2017).

51. R. Chen, M. Tian, S. Chen, W. Tian, G. H. Su, & S. Qiu, Three dimensional thermal hydraulic characteristic analysis of reactor core based on porous media method. Annals of Nuclear Energy, 104 (2017) 178–190.

52. S. Corzo, D. Ramajo, & N. Nigro, 1/3D modeling of the core coolant circuit of a PHWR nuclear power plant. Annals of Nuclear Energy, 83 (2015) 386–397.

53. G. Zhang, Y. H. Yang, H. Y. Gu, & Y. Q. Yu, Coolant distribution and mixing at the core inlet of PWR in a real geometry. Annals of Nuclear Energy, 60 (2013) 187-194.

54. R. Hu & T. H. Fanning, A momentum source model for wire-wrapped rod bundles - Concept, validation, and application. Nuclear Engineering and Design, 262 (2013) 371-389.

55. U. Bieder, V. Barthel, F. Ducros, & S. Vandroux, CFD Calculations of Wire Wrapped Fuel Bundles: Modeling and Validation Strategies. CFD4NRS-3 (Bethesda, USA, 2010), pp. 1-22.

56. F. Roelofs, V. R. Gopala, L. Chandra, M. Viellieber, & A. Class, Simulating fuel assemblies with low resolution CFD approaches. Nuclear Engineering and Design, 250 (2012) 548-559.

57. G. Class, M. O. Viellieber, A. Batta, & T. Fax, Coarse-Grid-CFD for pressure loss evaluation in rod bundles. Proc. ICAPP 2011 (Nice, France, 2011), pp. 1773–1780.

58. M. Viellieber & A. G. Class, Anisotropic porosity formulation of the coarse-grid-CFD (CGCFD). Proc. 2012 20th Int. Conf. Nucl. Eng. collocated with ASME 2012 Power Conf. ICONE20-POWER2012 (California, 2012), pp. 1–11.

59. N. Hanna, N. T. Dinh, R. W. Youngblood, & I. A. Bolotnov, Coarse-Grid Computational Fluid Dynamic (CG-CFD) Error Prediction using Machine Learning. arXiv preprint arXiv:1710.09105, (2017).

60. Y. Fournier, J. Bonelle, C. Moulinec, Z. Shang, A. G. Sunderland, & J. C. Uribe, Optimizing Code_Saturne computations on Petascale systems. Computers and Fluids, 45 (2011) 103–108.

61. B. L. Smith, C.-H. Song, S.-K. Chang, R. J. Lee, & J. W. Kim, Report of the OECD/NEA KAERI Rod Bundle CFD Benchmark Exercise. In: Report NEA/CSNI/R, (2013) 5.

62. N. E. Todreas & M. S. Kazimi, Nuclear Systems I: Thermal Hydraulic Fundamentals (1990).

63. W. Dittus & L.M.K. Boelter, Heat Transfer in Automobile Radiators of the Tubular Type. International Communications in Heat and Mass Transfer, 12 (1985) 3–22.

64. J. M. Creer, D. S. Rowe, J. M. Bates, & A. M. Sutey, Effects of Sleeve Blockages on Axial Velocity and Intensity of Turbulence in an Unheated 7 x 7 Rod Bundle. (1976) Battelle Pacific Northwest Labs.

65. Weiss & R. A. Markley, Open duct cooling-concept for the radial blanket region of a fast breeder reactor. Nuclear Engineering and Design, 16 (1971) 375–386.

66. S. J. Yoon, S. B. Kim, G. C. Park, H. Y. Yoon, & H. K. Cho, Application of Cupid for Subchannel-Scale Thermal-Hydraulic Analysis of Pressurized Water Reactor Core Under Single-Phase Conditions. Nuclear Engineering and Technology, 50 (2017) 54–67.

DOCUMENT INFORMATION

Project : Project FORTE - Nuclear Thermal Hydraulics Research & Development

Report Title : Smart Component Models for Nuclear Reactors

Client : Department for Business, Energy and Industrial Strategy (BEIS)

Report No. : FNC 53798/48650R

Issue No. : 1

Date : August 2019

Compiled By : Dr B Liu
(University of Sheffield)

Verified By : Professor S He
(University of Sheffield)

Approved By : C Howlett

Originating Office: FRAZER-NASH CONSULTANCY LIMITED
The Cube, 1 Lower Lamb Street, Bristol, BS1 5UD
T: +44 (0)117 9226242 F: +44 (0)117 9468924 W: www.fnc.co.uk

Frazer-Nash Consultancy Ltd
The Cube
1 Lower Lamb Street
Bristol
BS1 5UD

T +44 (0)117 9226242
F +44 (0)117 9468924

www.fnc.co.uk

Offices at:
Bristol, Burton-on-Trent, Dorchester,
Dorking, Glasgow, Plymouth, Warrington
and Adelaide